OPTIMIZATION STRATEGY OF REACTIVE POWER COMPENSATION IN GI - PV SYSTEM

Vaisakh P
PG Student
Department of EEE
Udaya School of Engineering
E-mail: vaisakhvkm@gmail.com

Abstract

Cascaded multilevel converter structure can be appealing for high-power solar photovoltaic (PV) systems thanks to its modularity, scalability, and distributed maximum power point tracking (MPPT). However, the power mismatch from cascaded individual PV converter modules can bring in voltage and system operation issues. This paper addresses these issues, explores the effects of reactive power compensation and optimization on system reliability and power quality, and proposes coordinated active and reactive power distribution to mitigate this issue. A vector method is first developed to illustrate the principle of power distribution. Accordingly, the relationship between power and voltage is analyzed with a wide operation range. Furthermore, a comprehensive control system with the RPCA is designed to achieve effective power distribution and dynamic voltage regulation. Simulation and experimental results are presented to demonstrate the effectiveness of the proposed reactive power compensation approach in grid-interactive cascaded PV systems.

Keywords: **Cascaded photovoltaic (PV) system, power–voltage distribution, reactive power compensation, unsymmetrical active power.**

1 INTRODUCTION

Worldwide renewable energy resources, especially solar energy, are growing dramatically in view of energy shortage and environmental concerns. Large-scale solar photovoltaic (PV) systems are typically connected to medium voltage distribution grids, where power converters are required to convert solar energy into electricity in such a grid-interactive PV system. To achieve direct medium-voltage grid access without using bulky medium-voltage transformer, cascaded multilevel converters are attracting more and more attraction due to their unique advantages such as enhanced energy harvesting capability implemented by distributed maximum power point tracking (MPPT), improved energy efficiency, lower cost, higher power density, scalability and modularity, plug-N-power operation, etc.

Although cascaded multilevel converters have been successfully introduced in medium- to high-voltage applications such as large motor drives, dynamic voltage restorers, reactive power compensations, and flexible ac transformation system devices, their applications in PV systems still face tough challenges because of solar power variability and the mismatch of maximum power point from each converter module due to manufacturing tolerances, partial shading, dirt, thermal gradients, etc. In a cascaded PV the output voltage from each converter module in one phase leg, which must fulfill grid codes or requirements, synthesizes system the total ac output voltage. Ideally, each converter module delivers the same active power to grid; hence, symmetrical voltage is distributed among these modules. In serious scenario, the synthesized output voltage may not be enough to meet the system requirement. As a result, the active power mismatch may not only result in losses in energy harvesting but also system instability and unreliability due to the inadequate output voltage or overmodulation issues.

A reactive power compensation algorithm (RPCA), which is inherently suitable for different types of cascaded PV system, is developed to improve system operation performance in view of point of common coupling voltage range and MPPT implementation.

2 LITERATURE REVIEW

Yan Zhou et al. (2013) developed a single-phase grid-connected photovoltaic (PV) module-integrated converter (MIC) based on cascaded quasi-Z-source inverters (qZSI). In this system, each qZSI module serves as an MIC and is connected to one PV panel. Due to the cascaded structure and qZSI topology, MIC features low-voltage gain requirement, single-stage energy conversion, enhanced reliability, and good output power quality. The enhancement mode gallium nitride field-effect transistors (eGaN FETs) are employed in the qZSI module for efficiency improvement at higher switching frequency. It is found that the qZSI is very suitable for the application of eGaN FETs because of the shoot-through capability.

Md. Rabiul Islam et al. (2014) evaluated that in solid-state semiconductors have led to the development of medium-voltage power converters (e.g., 6–36 kV), which could obviate the need for the step-up transformers of renewable power generation systems. The modular multi- level cascaded converters have been deemed as strong contenders for the development of medium-voltage converters, but the converters require multiple isolated and balanced dc supplies. Here a high-frequency link multilevel-cascaded medium-voltage converter is proposed. It is expected that the proposed new technology will have great potential for future renewable generation systems and smart grid applications.

Quan Li and Peter Wolfs evaluated that the annual world photovoltaic (PV) cell/module production is growing at almost an exponential rate and has reached 1727 MW in 2005. Building integrated PV (BIPV) projects are emerging as the strongest part of the PV market and grid interactive inverters are a key component in determining the total system cost.

Liming Liu, Hui Li Zhichao Wu and Yan Zhou (2011) developed a single-phase photovoltaic (PV) system integrating segmented energy storages (SES) using cascaded multilevel inverter. The system is designed to coordinate power allocation among PV, SES, and utility grid, mitigate the overvoltage at the point of common coupling (PCC), and achieve wide range reactive power compensation. The power allocation principle between PV and SES is described by a vector diagram, a sophisticated power allocation strategy is developed to allocate power between PV and SES based on a novel discrete Fourier transforms(DFT) phase-locked loop (PLL) method.

3 EXISTING METHOD

3.1 Introduction

Grid-connected high voltage high power (HVHP) PV system plays a major role in high penetration renewable energy systems. Cascaded multilevel inverter is very promising for the HVHP PV system due to its unique advantages such as lower electro-magnetic interference (EMI), independent maximum power point tracking (MPPT) for segmented PV arrays, transformer less topology, low rating devices application, etc.

3.2 Methodology

The PV system shown in Fig.3.2 includes n cascaded multilevel inverter modules for each phase, where each inverter module is connected to one unique dc-dc converter with high voltage insulation. The dc-dc converter is interfaced with individual PV arrays and therefore the independent MPPT can be achieved. Moreover, it is immune to double-line-frequency power ripple propagation into PV arrays. It can also solve the ground leakage current and PV insulation issues. The detailed dc-dc converter design with wide range input range would be presented. Here focused on the active and reactive control of the cascaded multilevel PV inverters. The selected PV application is a 3MW/12kV PV system. The n is selected to be 4 considering the trade off among the cost, lifetime, capacitors and switching devices

selection, switching frequency, and power quality. As a result, power rating of each inverter module is 250kW.

3.3 Block Diagram

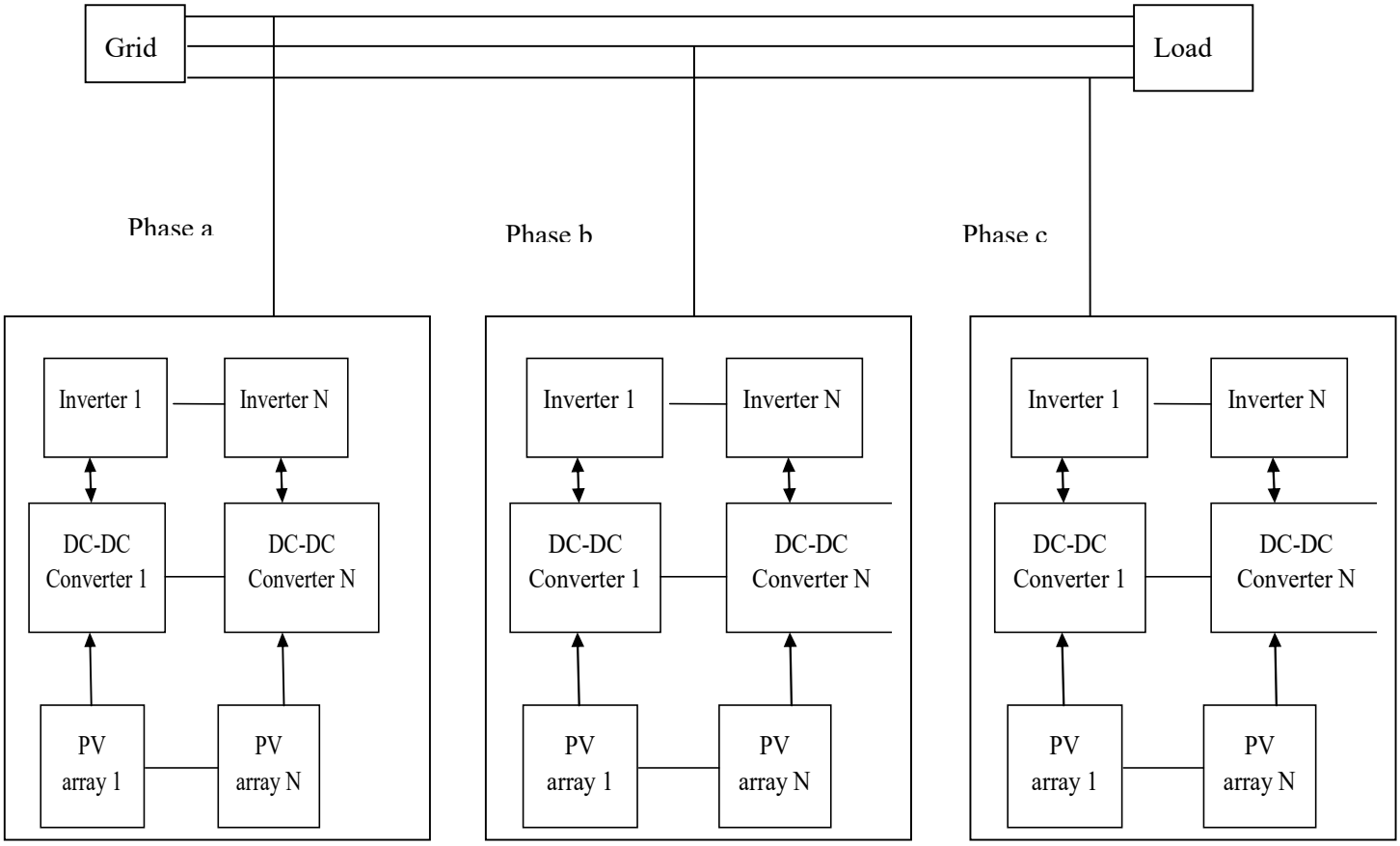

Figure 3.1: Block diagram of Grid-connected PV system with Cascaded PV inverters.

3.4 Power Distribution Strategy

Due to the cascaded topology, the same grid current will flow through the each inverter module in the same phase as shown in Fig.3.2. Therefore, the respective ac output voltage will decide the power distribution between these PV inverter modules. Vector diagrams are derived demonstrate the principle of power allocation between four PV inverter modules in phase a. Similarly, the analysis can be applied for phase b and phase c. Considering the relative stability of the grid voltage,$V_{ga}$is used for the synchronous signal. The α−axis is in phase with grid voltage and the β−axis lags the α−axis by 90° as shown in Fig.3.3 (a). The *d* axis is aligned with the grid voltage and the *q*−axis lags the *d*−axis by 90°.

$$V_{ga\_\alpha} = V_{ga}\sin(\omega t) \qquad (3.1)$$

$$V_{ga\_\beta} = -V_{ga}\cos(\omega t) \qquad (3.2)$$

Where the ω is the system line frequency,$V_{ga}$is the amplitude of the grid voltage,$V_{g\_d} = V_{ga}$, $V_{g\_q} = 0$. The grid current is relatively stable to the grid voltage in steady state. So the new *d* axis (*d'*) can be aligned with the grid current. As a result, the d' component of the inverter output voltage$V_{sa_d'}$determines the active power generation, and the q' component $V_{sa_q'}$decides the reactive power output. Fig.3.3 (b) describes clearly the power allocation between four PV inverter modules under different active power generation.

4 PROPOSED METHOD

4.1 System Configurations And Power Voltage Distribution

4.1.1 System Configuration

Fig. 4.1 describes the system configuration of one two-stage grid-interactive PV system with *n* cascaded converter modules for each phase, which is very suitable for the medium/high voltage application. It can be immune to the leakage current and PV potential induced degradation issues.

Here the three phase PV converters are connected in "wye" configuration. They also can be connected in "delta" configuration. In the two-stage PV system, the first-stage dc/dc converters with high voltage insulation can achieve the voltage boost and MPPT for the segmented PV arrays.

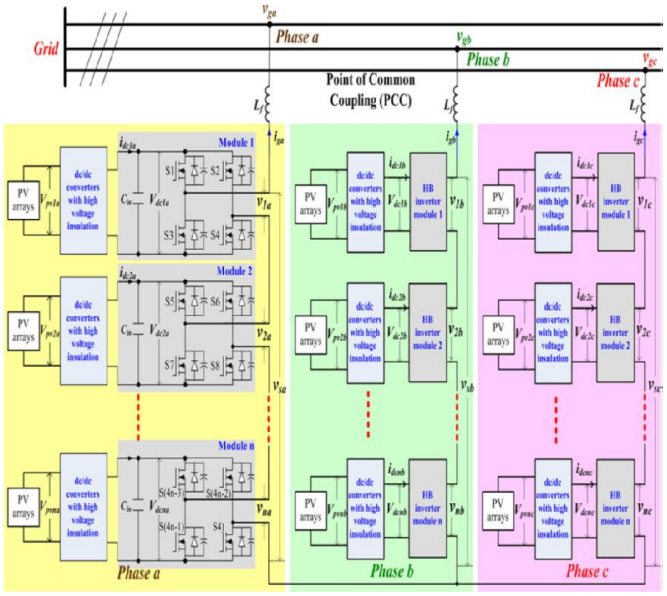

Figure 4.1: Grid-interactive PV system with cascaded PV converters.

The second stage three-level H-bridge converter modules are cascaded to augment the output voltage, deliver active power to grid, and provide reactive power compensation. In this case, improper power distribution and control are prone to an intrinsic instability problem if MPPT is still desired, which results in a limited operation range for the system. Moreover, it may also seriously deteriorate the system reliability and power quality. Particularly, appropriate reactive power compensation is very helpful to improve the operation of the cascaded PV system.

4.1.2 Power and Voltage Distribution Analysis

In the cascaded PV system, the same ac grid current flows through the ac side of each converter module. Therefore, the output voltage distribution of each module will determine the active and reactive power distribution. In order to clarify the power distribution, four modules are selected in the cascaded

PV converters in each phase as an example. Vector diagrams are derived in Fig. 3.2 to demonstrate the principle of power distribution between the cascaded converter modules in phase a.

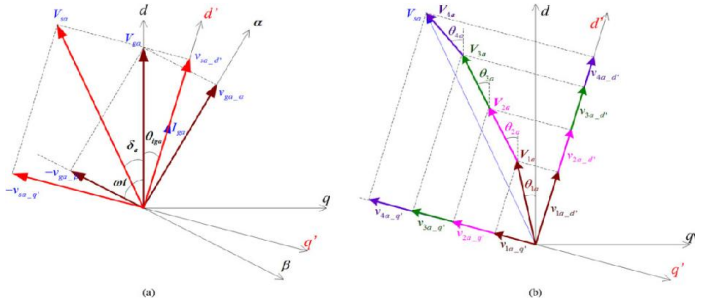

Figure 4.2: Vector diagrams showing relation between αβ frame, dq frame, and d_q_ frame. (a)Relationship between grid current, grid voltage, and converter output voltage in phase a. (b) Voltage distribution of the PV converter in phase a.

The same analysis can be extended to phase's b and c. It means that active and reactive power will be independently controlled in each phase. Therefore, a discrete Fourier transform phase locked Loop (PLL) method is adopted in this project, which is only based on single-phase grid voltage orientation and can extract fundamental phase, frequency, and amplitude information from any signal. Considering that the PCC voltage is relatively stable, $V_{ga}$is first used as the PLL synchronous signal of the cascaded PV system as shown in Fig. 3.2(a).$V_{ga}$is transformedinto $\alpha\beta$ stationary reference frame quantities $V_{ga\alpha}$and $V_{ga\beta}$which is the virtual voltage with $\pi/2$ phase shift to$V_{ga\alpha}$.

Fig. 3.2(b) illustrates voltage distribution of four cascaded converter modules under unsymmetrical active power generation in phase a. The output voltage of the total converter$V_{sa}$is synthesizedby the four-converter module output voltage with different amplitude and angles. The voltage components of each module in $d\_q\_$ frame, $V_{jad_}$and $V_{jaq\_}(j = 1, 2, \ldots,4)$, can be independently controlled to implement the decoupled active and reactive power control. Because of the same grid current through each convert module, the distributed $d\_$-axis and $q\_$-axis voltage components in $d\_q\_$ frame determine the active and reactive power distribution in these converter modules, respectively.

The average active and reactive power to grid in phase a, $P_{ga}$and P_{ga}, can be derived

$$P_{ga} - jQ_{ga} = \overrightarrow{V_{ga}} \left(\frac{\overrightarrow{V_{sa}} - \overrightarrow{V_{ga}}}{jX_L}\right)^* \qquad (1)$$

Where $_V_{ga}$is the vector of V_{ga},$_V_{sa}$is the vector of V_{sa}, $XL = \omega Lf$, ω is the fundamental radian frequency, and Lf is the grid filter inductor.

Considering the cascaded topology and modular structure,P_{ga}andQ_{ga}can also be expressed as shown bellow

$$\begin{cases} P_{ga} = \frac{1}{2}\frac{V_{sa}V_{ga}}{X_L}\sin\delta_a = \frac{1}{2}V_{ga}i_{ga-d} \\ \quad = \frac{1}{2}V_{sa-d'} \times \sqrt{i_{ga-d}^2 + i_{ga-q}^2} \\ Q_{ga} = -\frac{1}{2}\frac{V_{sa}V_{ga}}{X_L}\cos\delta_a + \frac{1}{2}\frac{V_{ga}^2}{X_L} = \frac{1}{2}V_{ga}i_{ga-q} \end{cases}$$

$$= \frac{1}{2} V_{sa-q'} \times \sqrt{i_{ga-d}^2 + i_{ga-q}^2} + \frac{1}{2} \left(i_{ga-d}^2 + i_{ga-q}^2\right) X_L \quad (2)$$

Where $_V_{ga}$is the magnitude of V_{ga},$_V_{sa}$is the magnitude ofV_{sa}, δa is phase angle between$V_{ga}$and V_{sa}, $i_{gad}$is the d-axis component of i_{ga}, and $i_{gaq}$is the q-axis component of i_{ga}.

A specific PV system application is selected to illustrate the relationship between active power, reactive power, and output voltage as shown in Figs. 3–6. In this application, the P_{ga}ratedis 1 MW, Lf is 0.8 mH, and the root mean square (RMS)value of line-line PCC voltage is 12 kV. $V_{sad_}$and$V_{saq_}$are normalized to clarify the aforementioned analysis, whichthe magnitude of phase-ground PCC voltage $V_{ga}$is defined as1.0 p.u. Fig. 4.3 and 4.4 illustrate the operation range of$V_{sas_}$ and$V_{saq_}$with k_1 and k_2 variation. Fig. 4.5 represents the operation range of $V_{sa}$with variedk_1 and k_2 .

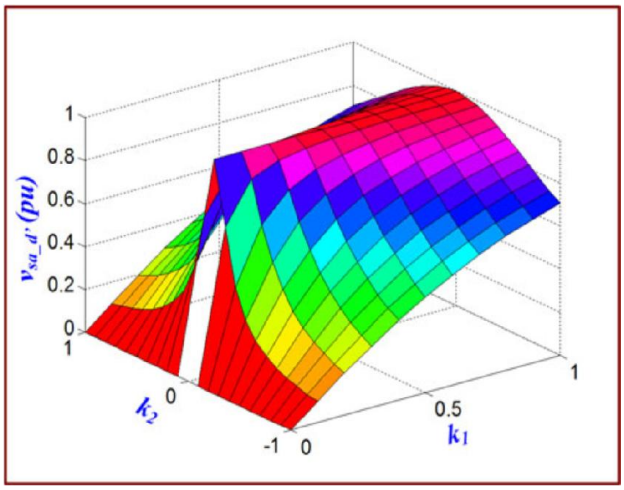

Figure 4.3: Operation range of $V_{sad\_}$ with respect to different active and reactive power to grid.

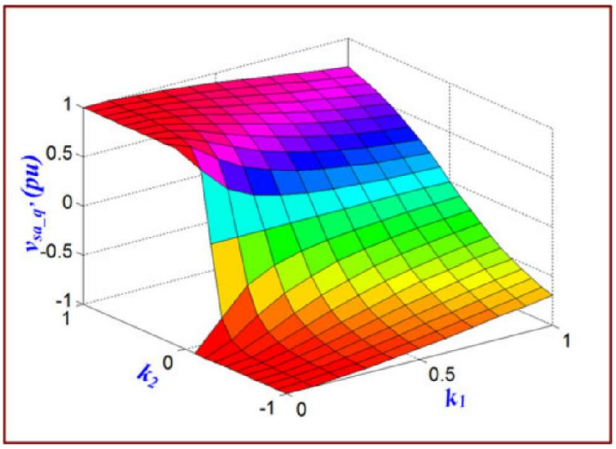

Figure 4.4: Operation range of $V_{saq\_}$ with respect to different active and reactivepower to grid.

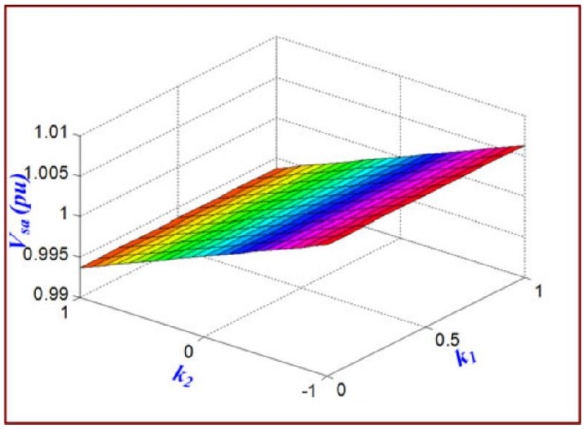

Figure 4.5: Operation range of Vsa with respect to different active and reactive power to grid.

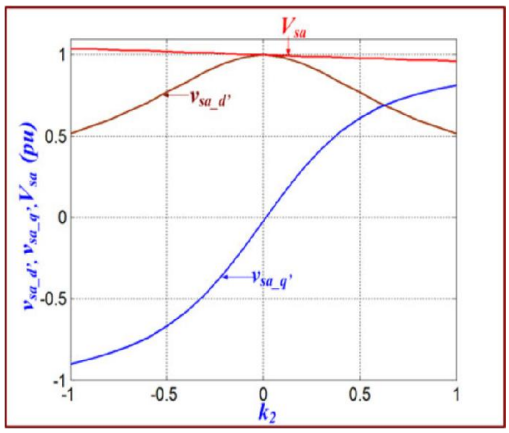

Figure 4.6: Relationship between $V_{sad\_}$, $V_{saq\_}$, andV_{sa} with fixed k_1 = 0.6and varied k_2.

It can be seen from Fig. 3.6 that $V_{sad_}$is gradually reduced withthe increase of reactive power. The reduced $V_{sad_}$is helpfulto reduce the burden of dc voltage. Fig. 4.7 shows an example with four cascaded converter modules to illustrate how reactive power compensation contributes to overcoming overmodulation caused by unsymmetrical active power in phase a. Their $d\_$-axis components are also the same, which is $V_{1ad\_}$= $V_{2ad\_}$=$V_{3ad\_}$= $V_{4ad\_}$. There is no reactive power requirement. These output voltage,V_{1a}− V_{4a}, are not more thantheir respective dc voltage. However, when the unsymmetrical active power is produced by these modules, for example, the active power from modules 1 and 2 is greater than ones from modules 3 and 4, over-modulation will happen. Without reactive power compensation,$V_{1a}$and V_{2a}will exceedtheir dc voltage, which results in overmodulation of the two modules output voltages. With the help of reactive power,$V_{1a}$and $V_{2a}$are brought back to the desired values, which are lessthan their dc voltage as shown in Fig. 4.7(c). The increase of$V_{saq_}$contribute to the reduction of $V_{sad\_}$, which ensures thatthe synthesized voltage of each module by their $d\_$-axis and $q\_$-axis components is no more than dc voltage. It is obvious that the system reliability can be further enhanced if the reactive power compensation with a wider range is allowed by grid codes.

In terms of the contribution of each module on $V_{sad_}$and $V_{saq\_}$, as well its dc linkvoltage, the output voltage of each PV converter module shouldbe subject to the following constraint:

$$\sqrt{\left(mp_{ja}V_{sa'_a}\right)^2 + (mq_{ja}V_{sa\_q'})^2} \leq V_{dcja} \text{ (j = 1,2,…..,n)} \qquad (3)$$

It can be seen from Fig. 4.8(a) that the available range of reactive power compensation is k_2=[−1,−0.6] when reactive power is injected into grid. There is no solutions satisfying the condition 4.6 for k_2=[−0.6, 0], where mq_{1a}= mq_{2a}= 0or mq_a<1 will both result in overmodulation. Considering the grid voltage, dc voltage ripple, and reactive power loss, the optimized voltage distribution at k_2 = −0.6 is selected asmq_{1a}= mq_{2a}= 0.15 and mq_{3a}= mq_{4a}= 0.35. Similarly, It can be seen from Fig. 4.8(b) that the available range of reactive power compensation is k_2=[0.58, 1] when reactive power is absorbed by the cascaded PV system. There are no solutions satisfying the condition (6) for k_2=[0, 0.58]. Considering the grid voltage, dc voltage ripple, and reactive power loss, an optimized voltage distribution at k_2= 0.7 is selected asmq_{1a}= mq_{2a}= 0.15 and mq_{3a}= mq_{4a}= 0.35.In this way, the reactive power distribution and compensation can be optimized.

4.2 Proposed Reactive Power Compensation Method

4.2.1 RPCA

As aforementioned, appropriate reactive power compensation will enhance the cascaded PV system reliability and improve power quality, especially for unsymmetrical active power generation. Fig.4.9 shows the proposed RPCA for the cascaded PV system in phase a. The same algorithm can be used in phase's b and c. The reactive power compensation requirement Q^*_{ga}isassociated with modulation index of output voltage from cascaded PV converter modules, PCC voltage, and MPPT control implementation which will determine the active power reference P^*_{ga}. In this scenario, $Q^*_{ga}$is zero and $P^*_{ga}$is derivedfrom the sum of maximum active power from the individual PV arrays $\sum_{j=1}^{n} P_{pvga}$subtracting power loss, which is defined as $k_1 P_{ga\_rated}$. Considering the known P_{ga_rated}, k_1 can be calculated as P^*_{ga}/P_{ga_rated}rated. It is determined by the MPPT control and dc voltage control.

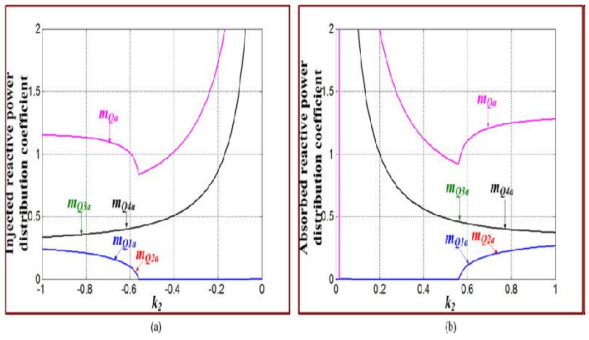

Figure 4.7: Voltage distribution among four cascaded converter modules with k_1 = 0.6 and k_2 changes. (a) Reactive power injection. (b) Reactive power absorption.

During the system operation, unsymmetrical active power may be generated from these modules due to PV module mismatch, orientation mismatch, partial shading, etc. Once the overmodulation is identified, the intentional reactive power compensation is activated to mitigate the overmodulation with grid code authorization.

If PCC voltage is high, maximum reactive power will be absorbed from grid to bring down the PCC voltage with the normal voltage range according to the IEEE Std. 1547, as well help possible MPPT implementation for each converter module simultaneously. k_2= 1 is designated to achieve the maximum reactive power absorption. The PV system operates like an inductor.

If the maximum reactive power compensation still cannot eliminate the overmodulation, MPPT control will be disabled to ensure the security and stability of the cascaded PV system. Instead, reactive power compensation can be optimized, that is the selection of k_2, to reduce the risk ofovervoltage or

undervoltage caused by the maximum reactivepower compensation. There are different ways to optimize reactivepower distribution in the cascaded PV converter modules.

4.2.2 Control System Design

A cascaded PV control system with the proposed RPCA in phase a is depicted in Fig. 4.10. The same control system is applied in phases b and c. Particularly, the proposed PRCA can be applied for any type of the cascaded PV system, such as single stage and two-stage PV system. The active and reactive power is regulated in the *dq* synchronous reference frame. PLL is used to synchronize the output voltage of the cascaded PV converters V_{sa}, grid current $i_{ga}$with V_{ga}so that the desired power control can be achieved. The RPCA provides the desired reactive powerQ^*_{ga}during unsymmetrical active power from the cascaded PV converter modules. The q-axis component command of grid current$i^*_{ga_q}$can be derived from the desiredQ^*_{ga}. The maximum active power harvesting from each module can be implemented by MPPT control and dc-link voltage control. In the one-stage cascaded PV system, the dc-link voltage referenceV^*_{dc} is obtained by theMPPT control for individual PV arrays.

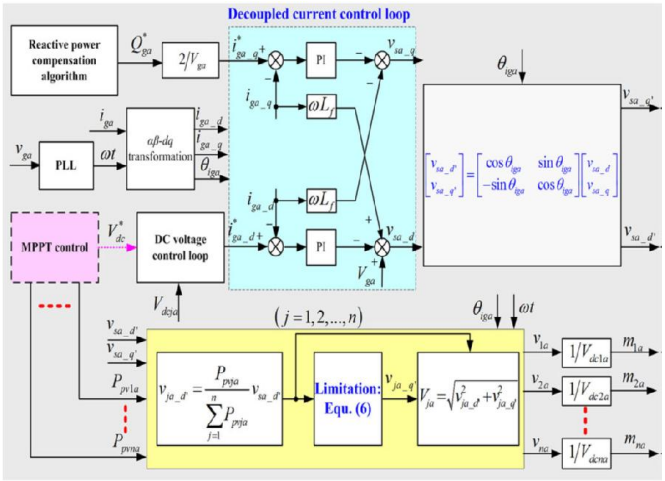

Figure 4.8: Block diagram of cascaded PV control system with the proposed RPCA in phase a.

In the two-stage cascaded PV system, V^*_{dc} is designatedbased on the grid voltage requirement. The V_{dcja}on each PVconverter module is controlled to track V^*_{dc} to generate the d axis component command of grid current $i^*_{ga\_d}$, which will coordinate the MPPT implementation. The active power from each module P_{pvga}can be obtained from the MPPT control. The modulation index of output voltage can be obtained by $m_{ja}=\frac{V_{ja}}{V_{dcja}}$.

4.3 Simulation Results

In order to explore the performance of grid-interactive cascaded PV system with the proposed reactive power compensation approach, simulations were first conducted in a co-simulation platform of MATLAB/Simulink and PSIM. A 3 MW/12 kV three-phase two-stage cascaded PV system as shown in Fig. 4.1 is applied to illustrate the active and reactive power distribution, grid voltage and current change, voltage distribution among four cascaded PV converter modules with reactive power injection and absorption during different scenarios in phase a, respectively. The grid current magnitude i_{ga}increasesfrom 40 A to 200 A. The system does not need the reactive power compensation because the symmetrical active power can equalize the output voltage from these modules. There is no overmodulation, and grid current and PCC voltage have good quality. The voltage and current waveforms before and after reactive power compensation optimization. The reactive power injection can improve system reliability but also increase the grid voltage magnitude$V_{ga}$from 9.7 to 10 kV. In order tolimit the

voltage rise, the optimized reactive power injection is reduced to −600 kVAR, that is, k_2 = −0.6 which is obtained from Fig. 4.8. In this case, the unsymmetrical reactive power is arranged between the four modules, Q_{1a}=Q_{2a}= −95 kVAR and Q_{3a}= Q_{4a}= −220 kVAR.

The power distribution with reactive power absorption considering the high grid voltage. The same active power as ones changes in each stage. At 1.5s, 1MVARreactive power Q_{ga}, that is, k_2= 1, is absorbed from grid toeliminate the overmodulation andQ_{1a}- $Q_{4a}$is controlled to thesame first.P_{ga}Keeps at 600 kW, which means that k_1= 0.6.Once the maximum active power P_{1a}- $P_{4a}$is accurately capturedat new steady system,Q_{1a}- $Q_{4a}$is rearranged to reducethe risk of undervoltage at 2 s.

6 RESULTS AND DISCUSSION

The experiments were conducted in the laboratory to verify the aforementioned theoretical analysis and the proposed reactive power compensation control performance. A two-stage cascaded PV system prototype with two 5 kW converter modules has been developed and the block scheme is given. The control algorithm is implemented in DSP + FPGA control platform. Considering the power loss, actual line impedance and grid equivalent impedance, per units in experiments, are a little different from ones in simulations. The loss on the filter inductor is provided by the PV system. The grid currenti_{ga}retrieves good quality and THD is 4.5%. However, the −1.4 kVAR reactive power compensation incurs the grid voltage V_{ga}increase from 280 to 290V. In order to avoid the overvoltage, the optimized reactive power compensation is introduced and Q_{ga}decreases from −1.4 to −1.1 kVAR. The reactive power distribution ratio between the two modules is 3:7 based on (4.3). The first module outputs high active power but provides less reactive power.

In order to ensure the safe and stable system operation, the maximum reactive power *Qga*= 1.45 kVAR is first absorbed from grid and the same reactive power $Q1a = Q2a$ = 700 VARis absorbed by the two modules as shown in Fig. 15(b). The loss on the filter inductor is provided by grid. The *iga* recovers good quality and THD is 4.68%. However, the 1.45 kVAR reactive power compensation incurs the grid voltage *Vga* decrease from 300 to 285 V.

6.1 SCREEN SHOT

Simulink Model

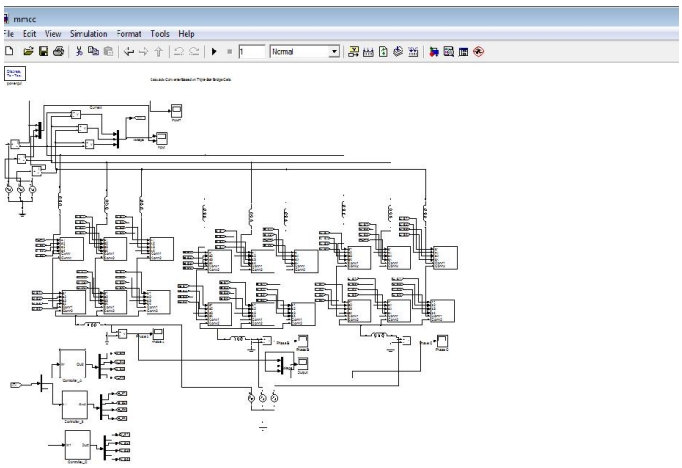

Input

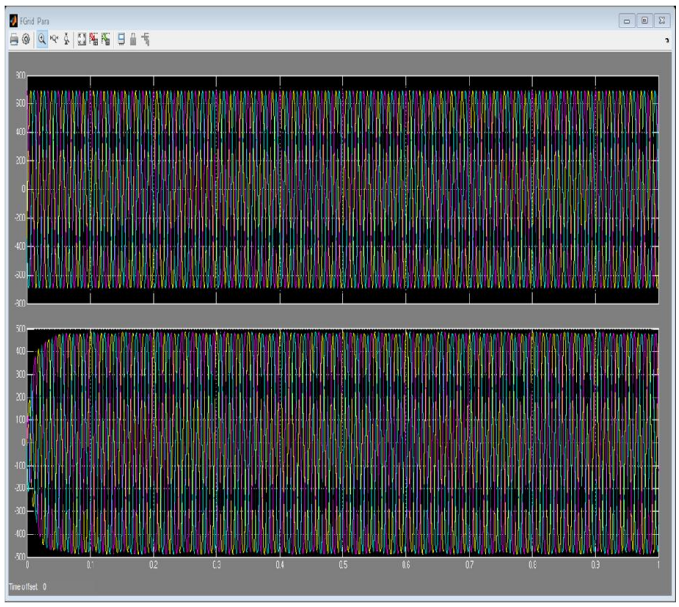

Output

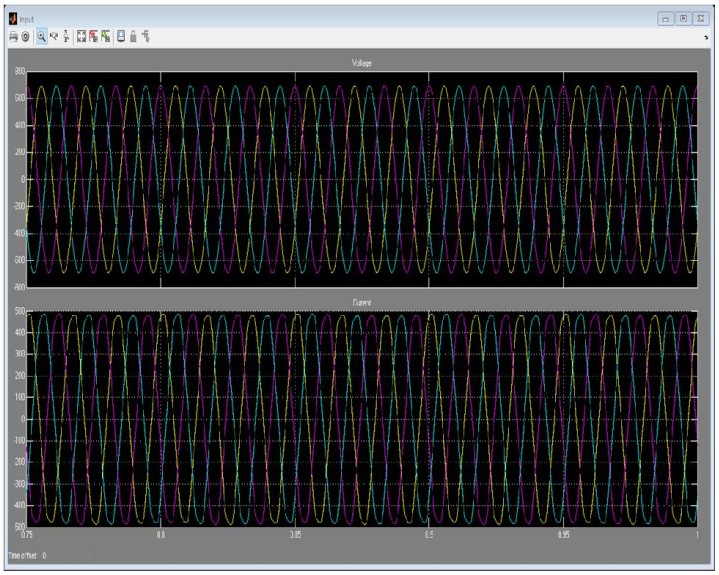

CONCLUSION

This paper addressed the effect of reactive power compensation on system operation performance in grid-interactive cascaded PV systems. The system stability and reliability issue caused by unsymmetrical active power was specifically analyzed. Reactive power compensation and distribution was introduced to mitigate this issue. The output voltage of each module was verified to directly determine the power distribution. The relationship between voltage distribution and power distribution

was illustrated with a wide power change range. An optimized RPCA was proposed considering the MPPT implementation, grid voltage, and overmodulation. Moreover, the RPAC was eligible to be integrated into different types of the cascaded PV system. Correspondingly, the control system with MPPT control and optimized RPCA was developed and validated by the simulation and experimental results under different scenarios. The proposed approach was demonstrated to be able to effectively enhance system operation stability and reliability, and improve power quality. In the future, the number of units can be extended up to 100.New test cases, such as the 26-unit or 52-unit systems, will be applied.

REFERENCES

[1] Y. Bo, L. Wuhua, Z. Yi, and H. Xiangning, "Design and analysis of a grid connected photovoltaic power system," *IEEE Trans. Power Electron.*,vol. 25, no. 4, pp. 992–1000, Apr. 2010.
[2] J. Ebrahimi, E. Babaei, and G. B. Gharehpetian, "A new topology of cascaded multilevel converters with reduced number of components for high-voltage applications," *IEEE Trans. Power Electron.*, vol. 26, no. 11,pp. 3109–3118, Nov. 2011.
[3] L. Nousiainen and J. Puukko, "Photovoltaic generator as an input source for power electronic converters," *IEEE Trans. Power Electron.*, vol. 28,no. 6, pp. 3028–3037, Jun. 2013.
[4] D. Meneses, F. Blaabjery, O. Garcia, and J. A. Cobos, "Review and comparison of step-up transformerless topologies for photovoltaic ac-module application," *IEEE Trans. Power Electron.*, vol. 28, no. 6, pp. 2649–2663,Jun. 2013.
[5] Y. Zhou, H. Li, and L. Liu, "Integrated autonomous voltage regulation and islanding detection for high penetration PV applications," *IEEE Trans .Power Electron.*, vol. 28, no. 6, pp. 2826–2841, Jun. 2013.
[6] J. Mei, B. Xiao, K. Shen, L. M. Tolbert, and J. Y. Zheng, "Modular multilevel inverter with new modulation method and its application to photovoltaic grid-connected generator," *IEEE Trans. Power Electron.*,vol. 28, no. 11, pp. 5063–5073, Nov. 2013.
[7] Y. Zhou, L. Liu, and H. Li, "A high performance photovoltaic module integrated converter (MIC) based on cascaded quasi-Z-source inverters(qZSI) using eGaN FETs," *IEEE Trans. Power Electron.*, vol. 28, no. 6,pp. 2727–2738, Jun. 2013.
[8] L. Liu, H. Li, and Y. Zhou, "A cascaded photovoltaic system integrating segmented energy storages with self-regulating power distribution control and wide range reactive power compensation," *IEEE Trans. Power Electron.*, vol. 26, no. 12, pp. 3545–3559, Dec. 2011.
[9] Q. Li and P. Wolfs, "A review of the single phase photovoltaic module integrated converter topologies with three different dc link configurations," *IEEE Trans. Power Electron.*, vol. 23, no. 3, pp. 1320–1333, May 2008.
[10] L. Zhang, K. Sun,Y. Xing, L. Feng, and H.Ge, "A modular grid-connected photovoltaic generation system based on dc bus," *IEEE Trans. Power Electron.*, vol. 26, no. 2, pp. 523–531, Feb. 2011.